



HAL
open science

Search for the lepton-flavour-violating decays

$$B^0_{\text{--}s} \rightarrow \tau^{\pm} \mu^{\mp} \text{ and } B^0 \rightarrow \tau^{\pm} \mu^{\mp}$$

Roel Aaij, Carlos Abellán Beteta, Bernardo Adeva, Marco Adinolfi, Christine Angela Aidala, Ziad Ajaltouni, Simon Akar, Pietro Albicocco, Johannes Albrecht, Federico Alessio, et al.

► To cite this version:

Roel Aaij, Carlos Abellán Beteta, Bernardo Adeva, Marco Adinolfi, Christine Angela Aidala, et al.. Search for the lepton-flavour-violating decays $B^0_{\text{--}s} \rightarrow \tau^{\pm} \mu^{\mp}$ and $B^0 \rightarrow \tau^{\pm} \mu^{\mp}$. Phys.Rev.Lett., 2019, 123 (21), pp.211801. 10.1103/PhysRevLett.123.211801 . hal-02148155

HAL Id: hal-02148155

<https://hal.science/hal-02148155>

Submitted on 23 Nov 2023

HAL is a multi-disciplinary open access archive for the deposit and dissemination of scientific research documents, whether they are published or not. The documents may come from teaching and research institutions in France or abroad, or from public or private research centers.

L'archive ouverte pluridisciplinaire **HAL**, est destinée au dépôt et à la diffusion de documents scientifiques de niveau recherche, publiés ou non, émanant des établissements d'enseignement et de recherche français ou étrangers, des laboratoires publics ou privés.



Search for the lepton-flavour-violating decays $B_s^0 \rightarrow \tau^\pm \mu^\mp$ and $B^0 \rightarrow \tau^\pm \mu^\mp$

LHCb collaboration

Abstract

Results are reported from a search for the rare decays $B_s^0 \rightarrow \tau^\pm \mu^\mp$ and $B^0 \rightarrow \tau^\pm \mu^\mp$, where the tau lepton is reconstructed in the channel $\tau^- \rightarrow \pi^- \pi^+ \pi^- \nu_\tau$. These processes are effectively forbidden in the standard model, but they can potentially occur at detectable rates in models of new physics that can induce lepton-flavour-violating decays. The search is based on a data sample corresponding to 3 fb^{-1} of proton-proton collisions recorded by the LHCb experiment in 2011 and 2012. The event yields observed in the signal regions for both processes are consistent with the expected standard model backgrounds. Because of the limited mass resolution arising from the undetected tau neutrino, the B_s^0 and B^0 signal regions are highly overlapping. Assuming no contribution from $B^0 \rightarrow \tau^\pm \mu^\mp$, the upper limit $\mathcal{B}(B_s^0 \rightarrow \tau^\pm \mu^\mp) < 4.2 \times 10^{-5}$ is obtained at 95% confidence level. If no contribution from $B_s^0 \rightarrow \tau^\pm \mu^\mp$ is assumed, a limit of $\mathcal{B}(B^0 \rightarrow \tau^\pm \mu^\mp) < 1.4 \times 10^{-5}$ is obtained at 95% confidence level. These results represent the first limit on $\mathcal{B}(B_s^0 \rightarrow \tau^\pm \mu^\mp)$ and the most stringent limit on $\mathcal{B}(B^0 \rightarrow \tau^\pm \mu^\mp)$.

Published in Phys. Rev. Lett. 123 (2019) 211801

© 2019 CERN for the benefit of the LHCb collaboration. CC-BY-4.0 licence.

Lepton-flavor-violating decays of mesons containing b quarks, such as $B^0(b\bar{d}) \rightarrow \tau^\pm\mu^\mp$ and $B_s^0(b\bar{s}) \rightarrow \tau^\pm\mu^\mp$, are extremely suppressed in the Standard Model (SM), with expected branching fractions of order 10^{-54} [1]. (The inclusion of charge-conjugate processes is implied throughout this Letter.) These processes involve not only quantum loops, but also neutrino oscillations. Signals at the level expected in the SM lie far below current and foreseen experimental sensitivities. However, many theoretical models proposed to explain possible experimental tensions observed in other B -meson decays (discussed below) naturally allow for branching fractions that are within current sensitivity. Among them, models containing a heavy neutral gauge boson (Z') could lead to a $B_s^0 \rightarrow \tau^\pm\mu^\mp$ branching fraction of up to 10^{-8} [2, 3] when only left-handed or right-handed couplings to quarks are considered, or of the order of 10^{-6} [3] if both are allowed. In models with either scalar or vector leptoquarks, the largest predictions for the $B_s^0 \rightarrow \tau^\pm\mu^\mp$ branching fraction range from 10^{-9} to 10^{-5} , depending on the assumed leptoquark mass [4–6]. The three-site Pati-Salam gauge model favours values for this branching fraction in the range 10^{-4} – 10^{-6} [7, 8].

The SM predicts that the electroweak couplings for the three lepton families are universal, a result referred to as Lepton Flavor Universality (LFU). Experimental tests of LFU performed using $b \rightarrow s\ell^+\ell^-$ and $b \rightarrow c\ell^-\bar{\nu}$ processes show tensions with respect to the SM predictions for the observables $R_{K^{(*)}}$ [9, 10] and $\mathcal{R}(D^{(*)})$ [11]. For the latter, the observed discrepancy with respect to the SM prediction is greater than 3 standard deviations. Because theoretical models that can account for the possible LFU effects observed in data often predict Lepton Flavor Violation (LFV) as well [12], searches for LFV processes provide a powerful signature for probing these models.

An upper limit $\mathcal{B}(B^0 \rightarrow \tau^\pm\mu^\mp) < 2.2 \times 10^{-5}$ at 90% confidence level (CL) was obtained by the BaBar collaboration [13]. There are currently no experimental results for the $B_s^0 \rightarrow \tau^\pm\mu^\mp$ mode.

This Letter reports results from the first search for the decay $B_s^0 \rightarrow \tau^\pm\mu^\mp$, along with the most stringent limit on the process $B^0 \rightarrow \tau^\pm\mu^\mp$. The analysis is performed on data corresponding to an integrated luminosity of 3 fb^{-1} of proton-proton (pp) collisions, recorded with the LHCb detector during the years 2011 and 2012 at centre-of-mass energies of 7 and 8 TeV, respectively. The τ leptons are reconstructed through the decay $\tau^- \rightarrow \pi^-\pi^+\pi^-\nu_\tau$, which mainly proceeds via the production of two intermediate resonances, $a_1(1260)^- \rightarrow \pi^+\pi^-\pi^-$ and $\rho(770)^0 \rightarrow \pi^+\pi^-$ [14], which help in the signal selection. In this mode, the τ decay vertex can be precisely reconstructed, facilitating a good reconstruction of the B -meson invariant mass despite the undetected neutrino. To avoid experimenter bias, the B -meson invariant-mass signal region was not examined until the selection and fit procedures were finalised. The signal yield is determined by performing an unbinned maximum-likelihood fit to the reconstructed B -meson invariant-mass distribution and is converted into a branching fraction using the decay $B^0 \rightarrow D^-(\rightarrow K^+\pi^-\pi^-)\pi^+$ as a normalisation channel.

The LHCb detector [15, 16] is a single-arm forward spectrometer covering the pseudorapidity range $2 < \eta < 5$, designed for the study of particles containing b or c quarks. The detector includes a high-precision tracking system consisting of a silicon-strip vertex detector surrounding the pp interaction region, a large-area silicon-strip detector located upstream of a dipole magnet with a bending power of about 4 Tm, and three stations of silicon-strip detectors and straw drift tubes placed downstream of the magnet. The tracking system provides a measurement of the momentum, p , of charged

particles with a relative uncertainty varying from 0.5% at low momentum to 1.0% at 200 GeV/ c . The minimum distance of a track to a primary vertex (PV), the impact parameter (IP), is measured with a resolution of $(15 + 29/p_T)$ μm , where p_T is the component of the momentum transverse to the beam, in GeV/ c . Different types of charged hadrons are distinguished using information from two ring-imaging Cherenkov detectors. Photons, electrons and hadrons are identified by a calorimeter system consisting of scintillating-pad and preshower detectors, an electromagnetic and a hadronic calorimeter. Muons are identified by a system composed of alternating layers of iron and multiwire proportional chambers.

The on-line event selection is performed by a trigger [17] consisting of a hardware stage based on information from the calorimeter and muon systems, followed by a software stage, which performs a full event reconstruction. At the hardware trigger stage, signal candidates are required to have a muon with high p_T , while, for the normalisation sample, events are required to have a hadron with high transverse energy in the calorimeters. The software trigger requires a two-, three-, or four-track secondary vertex with a significant displacement from any primary pp interaction vertex. A multivariate algorithm [18] is used to identify secondary vertices consistent with the decay of a b hadron. At least one charged particle must have a transverse momentum $p_T > 1.0$ (1.6) GeV/ c for muons (hadrons), and must be inconsistent with originating from a PV.

Simulation is used to optimise the selection, determine the signal model for the fit and obtain the selection efficiencies. In the simulation, pp collisions are generated using PYTHIA [19] with a specific LHCb configuration [20]. The τ decay is simulated using the TAUOLA decay library tuned with BaBar data [21], while the decays of all other unstable particles are described by EVTGEN [22]. Final-state radiation is accounted for using PHOTOS [23]. The interaction of the generated particles with the detector, and its response, are implemented using the GEANT4 toolkit [24], as described in Ref. [25].

Both signal and normalisation candidates are formed using tracks that are inconsistent with originating from any PV. Candidate $\tau^- \rightarrow \pi^- \pi^+ \pi^- \nu_\tau$ and $D^- \rightarrow K^+ \pi^- \pi^-$ decays are reconstructed from three tracks forming a good-quality vertex and with particle identification information corresponding to their assumed particle hypotheses. Candidate $B_{(s)}^0 \rightarrow \tau^\pm \mu^\mp$ decays are formed by combining a reconstructed τ lepton and an oppositely charged track identified as a muon. A control sample of same-sign candidates, which are formed by a τ lepton and a muon with identical charges, is also selected to serve, during the selection process, as a proxy for the large component of the background in which the muon and the tau candidate charges are uncorrelated. For the normalisation mode, $B^0 \rightarrow D^- \pi^+$ candidates are made out of a reconstructed D meson and an oppositely charged track identified as a pion. The decay vertex of the signal or normalisation B candidate is determined through a fit to all reconstructed particles in the decay chain [26], which is required to be of good quality. The B -meson p_T is required to be greater than 5 GeV/ c for both signal and normalisation modes.

While the neutrino from the τ decay escapes detection, its momentum vector can be constrained from the measured positions of the primary and τ decay vertices, the momenta of the muon and the three pions, and the trajectory of the muon. Then, by imposing the requirements that the mass of the system formed from the three pions and the unobserved neutrino corresponds to the mass of the tau lepton, and by requiring that the B decay vertex lies on the trajectories of the muon, of the tau lepton, and of the B meson, the invariant mass of the $B_{(s)}^0$ candidate can be determined analytically up to a

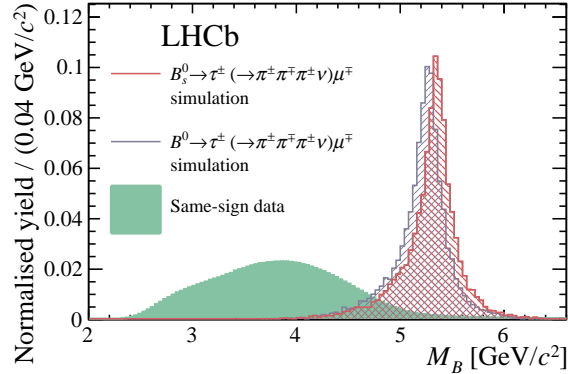


Figure 1: Normalized distributions of the reconstructed invariant mass for B_s^0 and B^0 in simulated event samples and for same-sign candidates in data, after applying the initial event selection (see the text).

twofold ambiguity. Because of the quadratic nature of the equation, the computed masses may be unphysical. This occurs in 32% of the selected signal in the simulated event sample due to measurement resolutions and in 48% of the same-sign candidates in data. These candidates are removed, thereby improving the signal-to-background ratio. The solution whose distribution shows the largest separation between signal and background is used as the reconstructed B invariant mass, M_B , in the analysis. The distributions of M_B for candidates satisfying the previously described initial selection in the simulated signal samples and in the opposite-sign control sample in the data are shown in Fig. 1.

To reduce the data to a manageable level and focus on the rejection of the most difficult backgrounds, the low-mass region with $M_B < 4 \text{ GeV}/c^2$ is discarded. The signal loss due to this requirement is negligible.

To further reduce the background, additional requirements, optimised with same-sign candidates and simulated samples, are applied to the selected $B_{(s)}^0 \rightarrow \tau^\pm \mu^\mp$ decays. Taking advantage of the resonant structure of the $\tau^- \rightarrow \pi^- \pi^+ \pi^- \nu_\tau$ decay, candidates with both combinations of oppositely charged pions with invariant-masses below $550 \text{ MeV}/c^2$ are removed. Candidates with a three-pion invariant mass greater than $1.8 \text{ GeV}/c^2$ are discarded to veto the background contribution due to $D^+ \rightarrow \pi^+ \pi^- \pi^+$ decays.

A set of isolation variables is used to reduce background from decays with additional reconstructed particles. The first class of isolation variables exploits the presence of activity in the calorimeter to identify the contribution of neutral particles contained in a cone centred on the B or τ flight directions. The second class is based on the presence of additional tracks consistent with originating from the B or τ decay vertices, or uses a multivariate classifier, trained on simulated data, to discriminate against candidates whose decay products are compatible with forming good-quality vertices with other tracks in the event. These variables are combined using a Boosted Decision Tree (BDT) [27], trained on same-sign candidates and simulated $B_s^0 \rightarrow \tau^\pm \mu^\mp$ decays. Candidates with a BDT output compatible with that of background are discarded. A second BDT is used to reduce to a negligible level the contribution of combinatorial background, which extends over the whole mass range but dominates at higher masses. It uses variables related to vertex quality and reconstructed particle opening angles and is trained on samples of same-sign candidates with $M_B > 6.2 \text{ GeV}/c^2$ and simulated $B_s^0 \rightarrow \tau^\pm \mu^\mp$ decays.

Some background processes, such as $B_{(s)}^0 \rightarrow D_{(s)}^- (\rightarrow \mu^- \bar{\nu}_\mu) \pi^+ \pi^- \pi^+$, have M_B distributions peaking in the signal region. In these decays, the three pions come from the B decay vertex, and therefore the reconstructed B and τ decay vertices are very close. Discarding candidates with a reconstructed τ decay-time significance lower than 1.8 reduces this type of background to a negligible level while keeping $\sim 75\%$ of signal, according to studies performed on simulation. All previously described selection criteria also suppress a possible contribution from the $B^0 \rightarrow a_1(1260)^- \mu^+ \nu_\mu$ mode, whose selection efficiency is 60 times lower than that of the signal. Its rate is currently unmeasured, but, given that the largest known $b \rightarrow u$ semileptonic decay branching fractions are of the order of 10^{-4} , its branching fraction is not expected to be much higher. Events from the decay $\tau^- \rightarrow \pi^- \pi^+ \pi^- \pi^0 \nu_\tau$ passing the selection are also included as signal.

The selection procedure retains 17 746 candidates. According to studies based on simulations, the remaining background is dominated by $B_{(s)}^0 \rightarrow D_{(s)}^{(*)} \mu \nu X$ decays.

The selection efficiencies for the signal and normalisation modes, $\epsilon_{B_{(s)}^0 \rightarrow \tau \mu}$ and $\epsilon_{B \rightarrow D\pi}$, respectively, are estimated using simulation or, whenever possible, data. The efficiency $\epsilon_{B_{(s)}^0 \rightarrow \tau \mu}$ includes those for both $\tau^- \rightarrow \pi^- \pi^+ \pi^- \nu_\tau$ and $\tau^- \rightarrow \pi^- \pi^+ \pi^- \pi^0 \nu_\tau$ decays, where the latter is weighted by the ratio of the two branching fractions. The $\tau^- \rightarrow \pi^- \pi^+ \pi^- \pi^0 \nu_\tau$ channel contributes by $\sim 16\%$ to the extracted signal yield. The tracking and particle identification efficiencies are determined using data [28, 29]. The trigger efficiency for the normalisation channel is estimated using a trigger-unbiased subsample made of events which have been triggered independently of the normalisation candidate. For the signal, muons from $B^+ \rightarrow J/\psi (\rightarrow \mu^+ \mu^-) K^+$ decays are used to evaluate the muon trigger efficiency and corrections are applied to the simulated signal samples. To account for differences between the control and the signal samples, the efficiency is computed as a function of the muon p_T and IP. Simulation as well as $B^+ \rightarrow J/\psi (\rightarrow \mu^+ \mu^-) K^+$ decays is used to determine the software-trigger efficiency and its systematic uncertainty.

The signal yield for the normalisation mode is obtained from a fit to the invariant-mass distribution of the $B^0 \rightarrow D^- \pi^+$ candidates. In the fit the signal is modelled by the sum of two Crystal Ball (CB) [30] functions, with tails on opposite sides, having common means and widths, but independent tail parameters. The tail parameters are fixed to values determined from a fit to a sample of $B^0 \rightarrow D^- (\rightarrow K^+ \pi^- \pi^-) \pi^+$ simulated decays, while all other parameters are left free. The small background contribution is described by an exponential function. The measured yield of the $B^0 \rightarrow D^- \pi^+$ mode is $N^{\text{norm}} = 22\,588 \pm 176$ where the uncertainty is statistical only.

The $B_{(s)}^0 \rightarrow \tau^\pm \mu^\mp$ branching fractions can be written as

$$\mathcal{B}(B_{(s)}^0 \rightarrow \tau^\pm \mu^\mp) = \alpha_{(s)}^{\text{norm}} \cdot N_{(s)}^{\text{sig}}, \quad (1)$$

where $N_{(s)}^{\text{sig}}$ is the number of observed $B_{(s)}^0 \rightarrow \tau^\pm \mu^\mp$ decays and $\alpha_{(s)}^{\text{norm}}$ a normalisation factor. The latter is defined by

$$\alpha_{(s)}^{\text{norm}} = \frac{f_{B^0}}{f_{B_{(s)}^0}} \cdot \frac{\mathcal{B}(B^0 \rightarrow D^- (\rightarrow K^+ \pi^- \pi^-) \pi^+)}{\mathcal{B}(\tau^- \rightarrow \pi^- \pi^+ \pi^- \nu_\tau)} \cdot \frac{\epsilon_{B \rightarrow D\pi}}{\epsilon_{B_{(s)}^0 \rightarrow \tau \mu}} \cdot \frac{1}{N^{\text{norm}}}, \quad (2)$$

using externally measured quantities: the ratio of b -quark hadronisation fractions to B_s^0 and B^0 mesons, $f_{B_s^0}/f_{B^0} = 0.259 \pm 0.015$ [31], $\mathcal{B}(B^0 \rightarrow D^- (\rightarrow K^+ \pi^- \pi^-) \pi^+) = (2.26 \pm$

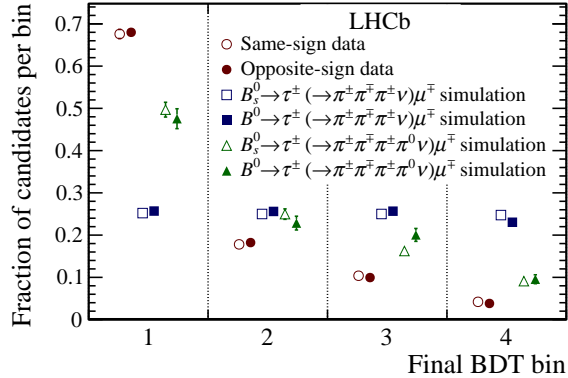


Figure 2: Final BDT output binned distributions for data and simulated signal samples. The markers are displaced horizontally to improve visibility.

$0.14) \times 10^{-4}$ [32] and $\mathcal{B}(\tau^- \rightarrow \pi^- \pi^+ \pi^- \nu_\tau) = (9.02 \pm 0.05)\%$ [32]. The measured values of $\alpha_{(s)}^{\text{norm}}$ for the B_s^0 and B^0 modes are, respectively,

$$\begin{aligned} \alpha_s^{\text{norm}} &= (4.32 \pm 0.19 \pm 0.45 \pm 0.36) \times 10^{-7} \text{ and} \\ \alpha^{\text{norm}} &= (1.25 \pm 0.06 \pm 0.13 \pm 0.08) \times 10^{-7}, \end{aligned} \quad (3)$$

where the three quoted uncertainties are the statistical uncertainty due to the sizes of the signal and normalisation simulated and data samples, the systematic uncertainty on the selection efficiencies (dominated by the trigger efficiency contribution, $\sim 11\%$) and the total uncertainty on the externally measured quantities.

A final BDT is built to split the selected candidates into four samples with different signal-to-background ratios. It combines 16 discriminating variables, none of which are correlated with the B -meson invariant mass. The most important ones are the invariant masses of the three-pion system and of the two combinations of oppositely charged pions, the B -meson IP and flight distance significances, and the output of the BDT based on isolation variables. The output of the BDT is transformed to have a uniform distribution between 0 and 1 for $B_s^0 \rightarrow \tau^\pm (\rightarrow \pi^\pm \pi^\mp \pi^\pm \nu_\tau) \mu^\mp$ simulated decays. As a consequence, its distribution for the background peaks at low BDT values. All samples are divided into four bins of equal width in BDT output. Their distributions are shown in Fig. 2.

The signal yield is evaluated by performing a simultaneous unbinned maximum-likelihood fit to the M_B distributions in the range $[4.6, 5.8] \text{ GeV}/c^2$ of the four samples corresponding to different BDT bins. In each bin, the data are described by the sum of a signal and a background component. The background shape is modelled by the upper tail of a reversed CB function, whose peak position and tail parameters are shared among BDT bins. For the determination of the systematic uncertainties, different sets of constrained parameters or alternative background models, such as the sum of two Gaussian functions, are considered. The signal shapes are described by double-sided Hypatia functions [33] whose parameters are initialized to the values obtained from a fit to the $B_s^0 \rightarrow \tau^\pm \mu^\mp$ and $B^0 \rightarrow \tau^\pm \mu^\mp$ simulated samples and allowed to vary within Gaussian constraints accounting for possible discrepancies between data and simulation. The width of the Hypatia functions are $\sim 330 \text{ MeV}/c^2$ for both signal modes in the most sensitive BDT bin. As the separation between $B_s^0 \rightarrow \tau^\pm \mu^\mp$ and $B^0 \rightarrow \tau^\pm \mu^\mp$ signal shapes is limited, two independent fits are performed while assuming the contribution of either the B_s^0 or

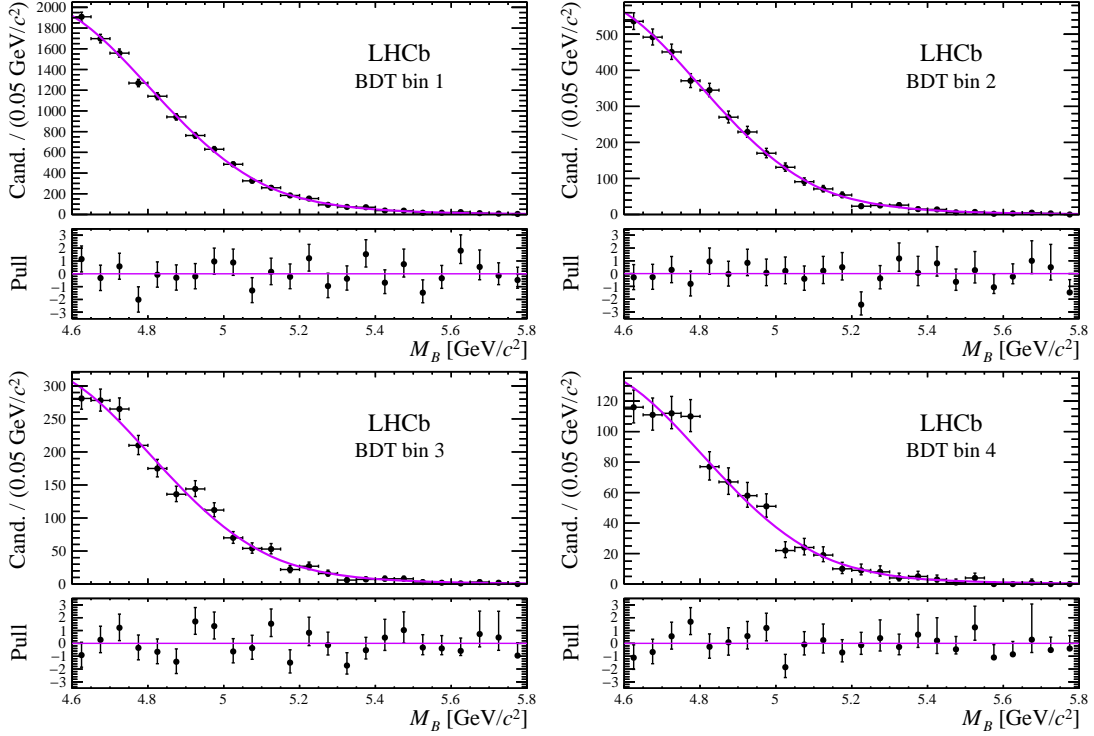


Figure 3: Distributions of the reconstructed B invariant-mass in data in the four final BDT bins with the projections of the fit for the B_s^0 signal-only hypothesis overlaid. The lower-part of each figure shows the normalised residuals.

the B^0 signal only. The signal fractional yields in each BDT bin are Gaussian constrained according to their expected values and uncertainties. The fit result corresponding to the hypothesis of the B_s^0 signal only is shown in Fig. 3. The fit procedure is validated by performing fits to a set of pseudoexperiments where the mass distributions are randomly generated according to the background model observed in the data. The pulls of all fitted parameters are normally distributed except those of the signal yields N^{sig} , which have the expected widths but exhibit a very small bias of -3 ± 1 (2 ± 2) events for the B_s^0 (B^0) mode. This effect is accounted for by adding the bias to N^{sig} in the simultaneous fits to the four BDT regions for both B^0 and B_s^0 . The obtained signal yields are

$$\begin{aligned}
 N_{B_s^0 \rightarrow \tau^\pm \mu^\mp}^{\text{sig}} &= -16 \pm 38 \text{ and} \\
 N_{B^0 \rightarrow \tau^\pm \mu^\mp}^{\text{sig}} &= -65 \pm 58,
 \end{aligned}$$

where the uncertainties account for the statistical ones as well as those on the signal and background shape parameters. They show no evidence of any signal excess.

Using the calculated values of the normalisation factors α^{norm} and α_s^{norm} from Eq. 1 together with Eq. 3, the observed yields from the likelihood fits are translated into upper limits on the branching fractions using the CLs method [34, 35]. The total uncertainty on the normalisation factor is accounted for as an additional Gaussian constraint in the simultaneous fit. Furthermore, a systematic uncertainty on the signal yield of 34 (41) for the B_s^0 (B^0) mode, derived using different sets of constrained parameters or alternative

Table 1: Expected and observed 90% and 95% CL limits on the $B_{(s)}^0 \rightarrow \tau^\pm \mu^\mp$ branching fraction.

Mode	Limit	90% CL	95% CL
$B_s^0 \rightarrow \tau^\pm \mu^\mp$	Observed	3.4×10^{-5}	4.2×10^{-5}
	Expected	3.9×10^{-5}	4.7×10^{-5}
$B^0 \rightarrow \tau^\pm \mu^\mp$	Observed	1.2×10^{-5}	1.4×10^{-5}
	Expected	1.6×10^{-5}	1.9×10^{-5}

background models, is added to account for the uncertainties in the background shape. The expected and observed CLs values as a function of the branching fraction are shown in the Supplemental Material [36]. The corresponding limits on the B_s^0 and B^0 branching fractions at 90% and 95% CL are given in Table 1 assuming negligible contribution from the $B^0 \rightarrow a_1(1260)^- \mu^+ \nu_\mu$ mode. A possible residual contribution of this background would lower the expected limits by $\sim 16\% \times (\mathcal{B}(B^0 \rightarrow a_1(1260)^- \mu^+ \nu_\mu)/10^{-4})$. The impact of systematic uncertainties on the final limits is about 35%, dominated by the uncertainty on the background model.

These results represent the best upper limits to date. They constitute a factor ~ 2 improvement with respect to the BaBar result for the B^0 mode [13] and the first measurement for the B_s^0 mode. The allowed range on the $B_s^0 \rightarrow \tau^\pm \mu^\mp$ branching fraction preferred by the three-site Pati-Salam model [7, 8] is significantly reduced by the results presented in this Letter.

Acknowledgements

We express our gratitude to our colleagues in the CERN accelerator departments for the excellent performance of the LHC. We thank the technical and administrative staff at the LHCb institutes. We acknowledge support from CERN and from the national agencies: CAPES, CNPq, FAPERJ and FINEP (Brazil); MOST and NSFC (China); CNRS/IN2P3 (France); BMBF, DFG and MPG (Germany); INFN (Italy); NWO (Netherlands); MNiSW and NCN (Poland); MEN/IFA (Romania); MSHE (Russia); MinECo (Spain); SNSF and SER (Switzerland); NASU (Ukraine); STFC (United Kingdom); DOE NP and NSF (USA). We acknowledge the computing resources that are provided by CERN, IN2P3 (France), KIT and DESY (Germany), INFN (Italy), SURF (Netherlands), PIC (Spain), GridPP (United Kingdom), RRCKI and Yandex LLC (Russia), CSCS (Switzerland), IFIN-HH (Romania), CBPF (Brazil), PL-GRID (Poland) and OSC (USA). We are indebted to the communities behind the multiple open-source software packages on which we depend. Individual groups or members have received support from AvH Foundation (Germany); EPLANET, Marie Skłodowska-Curie Actions and ERC (European Union); ANR, Labex P2IO and OCEVU, and Région Auvergne-Rhône-Alpes (France); Key Research Program of Frontier Sciences of CAS, CAS PIFI, and the Thousand Talents Program (China); RFBR, RSF and Yandex LLC (Russia); GVA, XuntaGal and GENCAT (Spain); the Royal Society and the Leverhulme Trust (United Kingdom).

References

- [1] L. Calibbi and G. Signorelli, *Charged lepton flavour violation: an experimental and theoretical introduction*, Riv. Nuovo Cim. **41** (2018) 1, [arXiv:1709.00294](#).
- [2] D. Bečirević, O. Sumensari, and R. Z. Funchal, *Lepton flavor violation in exclusive $b \rightarrow s$ decays*, Eur. Phys. J. C **76** (2016) 134, [arXiv:1602.00881](#).
- [3] A. Crivellin *et al.*, *Lepton-flavor violating B decays in generic Z' models*, Phys. Rev. D **92** (2015) 054013, [arXiv:1504.07928](#).
- [4] I. de Medeiros Varzielas and G. Hiller, *Clues for flavor from rare lepton and quark decays*, JHEP **6** (2015) 72, [arXiv:1503.01084](#).
- [5] D. Bečirević, N. Košnik, O. Sumensari, and R. Zukanovich Funchal, *Palatable leptoquark scenarios for lepton flavor violation in exclusive $b \rightarrow sl_1l_2$ modes*, JHEP **11** (2016) 035, [arXiv:1608.07583](#).
- [6] A. D. Smirnov, *Vector leptoquark mass limits and branching ratios of K_L^0 , B^0 , $B_s \rightarrow l_i^+l_j^-$ decays with account of fermion mixing in leptoquark currents*, Mod. Phys. Lett. A **33** (2018) 1850019, [arXiv:1801.02895](#).
- [7] M. Bordone, C. Cornella, J. Fuentes-Martín, and G. Isidori, *Low-energy signatures of the PS^3 model: from B -physics anomalies to LFV*, JHEP **2018** (2018) 148, [arXiv:1805.09328](#).
- [8] C. Cornella, J. Fuentes-Martin, and G. Isidori, *Revisiting the vector leptoquark explanation of the B -physics anomalies*, [arXiv:1903.11517](#).
- [9] LHCb collaboration, R. Aaij *et al.*, *Test of lepton universality with $B^0 \rightarrow K^{*0}\ell^+\ell^-$ decays*, JHEP **08** (2017) 055, [arXiv:1705.05802](#).
- [10] LHCb collaboration, R. Aaij *et al.*, *Search for lepton-universality violation in $B^+ \rightarrow K^+\ell^+\ell^-$ decays*, [arXiv:1903.09252](#), to appear in Phys. Rev. Lett.
- [11] Heavy Flavor Averaging Group, Y. Amhis *et al.*, *Averages of b -hadron, c -hadron, and τ -lepton properties as of summer 2016*, Eur. Phys. J. **C77** (2017) 895, [arXiv:1612.07233](#), updated results and plots available at <https://hflav.web.cern.ch>.
- [12] S. L. Glashow, D. Guadagnoli, and K. Lane, *Lepton flavor violation in B decays?*, Phys. Rev. Lett. **114** (2015) 091801, [arXiv:1411.0565](#).
- [13] BaBar collaboration, B. Aubert *et al.*, *Searches for the decays $B^0 \rightarrow \ell^\pm\tau^\mp$ and $B^+ \rightarrow \ell^+\nu$ ($\ell=e, \mu$) using hadronic tag reconstruction*, Phys. Rev. **D77** (2008) 091104, [arXiv:0801.0697](#).
- [14] ALEPH collaboration, S. Schael *et al.*, *Branching ratios and spectral functions of τ decays: Final ALEPH measurements and physics implications*, Phys. Rept. **421** (2005) 191, [arXiv:hep-ex/0506072](#).

- [15] LHCb collaboration, A. A. Alves Jr. *et al.*, *The LHCb detector at the LHC*, JINST **3** (2008) S08005.
- [16] LHCb collaboration, R. Aaij *et al.*, *LHCb detector performance*, Int. J. Mod. Phys. **A30** (2015) 1530022, arXiv:1412.6352.
- [17] R. Aaij *et al.*, *The LHCb trigger and its performance in 2011*, JINST **8** (2013) P04022, arXiv:1211.3055.
- [18] V. V. Gligorov and M. Williams, *Efficient, reliable and fast high-level triggering using a bonsai boosted decision tree*, JINST **8** (2013) P02013, arXiv:1210.6861.
- [19] T. Sjöstrand, S. Mrenna, and P. Skands, *PYTHIA 6.4 physics and manual*, JHEP **05** (2006) 026, arXiv:hep-ph/0603175; T. Sjöstrand, S. Mrenna, and P. Skands, *A brief introduction to PYTHIA 8.1*, Comput. Phys. Commun. **178** (2008) 852, arXiv:0710.3820.
- [20] I. Belyaev *et al.*, *Handling of the generation of primary events in Gauss, the LHCb simulation framework*, J. Phys. Conf. Ser. **331** (2011) 032047.
- [21] I. M. Nugent *et al.*, *Resonance chiral Lagrangian currents and experimental data for $\tau^- \rightarrow \pi^- \pi^- \pi^+ \nu_\tau$* , Phys. Rev. D **88** (2013) 093012, arXiv:1310.1053.
- [22] D. J. Lange, *The EvtGen particle decay simulation package*, Nucl. Instrum. Meth. **A462** (2001) 152.
- [23] P. Golonka and Z. Was, *PHOTOS Monte Carlo: A precision tool for QED corrections in Z and W decays*, Eur. Phys. J. **C45** (2006) 97, arXiv:hep-ph/0506026.
- [24] Geant4 collaboration, J. Allison *et al.*, *Geant4 developments and applications*, IEEE Trans. Nucl. Sci. **53** (2006) 270; Geant4 collaboration, S. Agostinelli *et al.*, *Geant4: A simulation toolkit*, Nucl. Instrum. Meth. **A506** (2003) 250.
- [25] M. Clemencic *et al.*, *The LHCb simulation application, Gauss: Design, evolution and experience*, J. Phys. Conf. Ser. **331** (2011) 032023.
- [26] W. D. Hulsbergen, *Decay chain fitting with a Kalman filter*, Nucl. Instrum. Meth. **A552** (2005) 566, arXiv:physics/0503191.
- [27] L. Breiman, J. H. Friedman, R. A. Olshen, and C. J. Stone, *Classification and regression trees*, Wadsworth international group, Belmont, California, USA, 1984.
- [28] LHCb collaboration, R. Aaij *et al.*, *Measurement of the track reconstruction efficiency at LHCb*, JINST **10** (2015) P02007, arXiv:1408.1251.
- [29] L. Anderlini *et al.*, *The PIDCalib package*, LHCb-PUB-2016-021, 2016.
- [30] T. Skwarnicki, *A study of the radiative cascade transitions between the Upsilon-prime and Upsilon resonances*, PhD thesis, Institute of Nuclear Physics, Krakow, 1986, DESY-F31-86-02.

- [31] LHCb collaboration, R. Aaij *et al.*, *Measurement of the fragmentation fraction ratio f_s/f_d and its dependence on B meson kinematics*, JHEP **04** (2013) 001, [arXiv:1301.5286](#), f_s/f_d value updated in LHCb-CONF-2013-011.
- [32] Particle Data Group, M. Tanabashi *et al.*, *Review of particle physics*, Phys. Rev. **D98** (2018) 030001.
- [33] D. Martínez Santos and F. Dupertuis, *Mass distributions marginalized over per-event errors*, Nucl. Instrum. Meth. **A764** (2014) 150, [arXiv:1312.5000](#).
- [34] A. L. Read, *Presentation of search results: The $CL(s)$ technique*, J. Phys. **G28** (2002) 2693.
- [35] G. Cowan, K. Cranmer, E. Gross and O. Vitells, *Asymptotic formulae for likelihood-based tests of new physics*, Eur. Phys. J. C **71** (2011) .
- [36] See Supplemental Material.

Supplemental material for LHCb-PAPER-2019-016

Figures 4 and 5 show the expected and observed CLs values as a function of the $B_s^0 \rightarrow \tau^\pm \mu^\mp$ and $B^0 \rightarrow \tau^\pm \mu^\mp$ branching fractions.

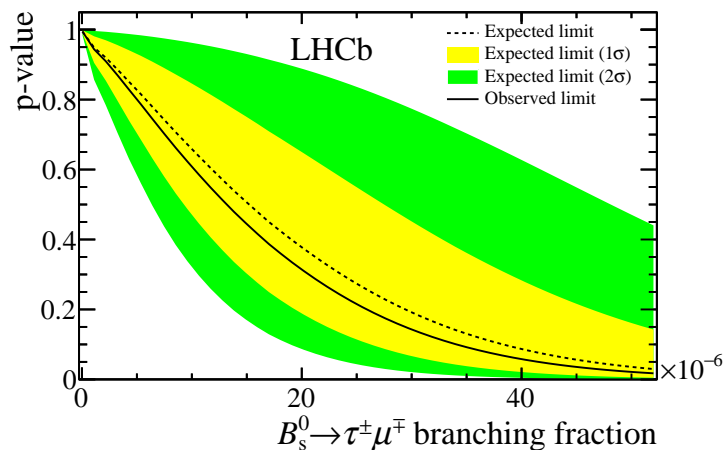


Figure 4: The expected and observed p-values derived with the CLs method as a function of the $B_s^0 \rightarrow \tau^\pm \mu^\mp$ branching fraction.

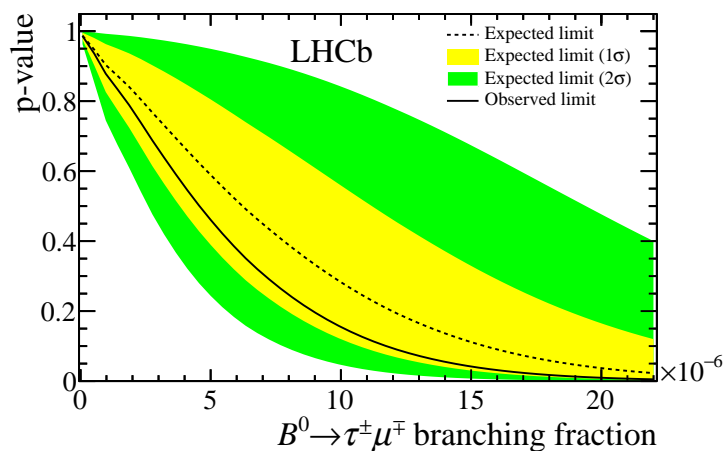


Figure 5: The expected and observed p-values derived with the CLs method as a function of the $B^0 \rightarrow \tau^\pm \mu^\mp$ branching fraction.

LHCb collaboration

R. Aaij³⁰, C. Abellán Beteta⁴⁷, B. Adeva⁴⁴, M. Adinolfi⁵¹, C.A. Aidala⁷⁸, Z. Ajaltouni⁸, S. Akar⁶², P. Albicocco²¹, J. Albrecht¹³, F. Alessio⁴⁵, M. Alexander⁵⁶, A. Alfonso Alberio⁴³, G. Alkhazov³⁶, P. Alvarez Cartelle⁵⁸, A.A. Alves Jr⁴⁴, S. Amato², Y. Amhis¹⁰, L. An²⁰, L. Anderlini²⁰, G. Andreassi⁴⁶, M. Andreotti¹⁹, J.E. Andrews⁶³, F. Archilli²¹, J. Arnau Romeu⁹, A. Artamonov⁴², M. Artuso⁶⁵, K. Arzymatov⁴⁰, E. Aslanides⁹, M. Atzeni⁴⁷, B. Audurier²⁵, S. Bachmann¹⁵, J.J. Back⁵³, S. Baker⁵⁸, V. Balagura^{10,b}, W. Baldini^{19,45}, A. Baranov⁴⁰, R.J. Barlow⁵⁹, S. Barsuk¹⁰, W. Barter⁵⁸, M. Bartolini^{22,h}, F. Baryshnikov⁷⁴, V. Batozskaya³⁴, B. Batsukh⁶⁵, A. Battig¹³, V. Battista⁴⁶, A. Bay⁴⁶, F. Bedeschi²⁷, I. Bediaga¹, A. Beiter⁶⁵, L.J. Bel³⁰, V. Belavin⁴⁰, S. Belin²⁵, N. Belyi⁴, V. Bellee⁴⁶, K. Belous⁴², I. Belyaev³⁷, G. Bencivenni²¹, E. Ben-Haim¹¹, S. Benson³⁰, S. Beranek¹², A. Berezhnoy³⁸, R. Bernet⁴⁷, D. Berninghoff¹⁵, H.C. Bernstein⁶⁵, E. Bertholet¹¹, A. Bertolin²⁶, C. Betancourt⁴⁷, F. Betti^{18,e}, M.O. Bettler⁵², I.a. Bezshyiko⁴⁷, S. Bhasin⁵¹, J. Bhom³², M.S. Bieker¹³, S. Bifani⁵⁰, P. Billoir¹¹, A. Birnkraut¹³, A. Bizzeti^{20,u}, M. Bjørn⁶⁰, M.P. Blago⁴⁵, T. Blake⁵³, F. Blanc⁴⁶, S. Blusk⁶⁵, D. Bobulska⁵⁶, V. Bocci²⁹, O. Boente Garcia⁴⁴, T. Boettcher⁶¹, A. Bondar^{41,w}, N. Bondar³⁶, S. Borghi^{59,45}, M. Borisyak⁴⁰, M. Borsato¹⁵, M. Boubdir¹², T.J.V. Bowcock⁵⁷, C. Bozzi^{19,45}, S. Braun¹⁵, A. Brea Rodriguez⁴⁴, M. Brodski⁴⁵, J. Brodzicka³², A. Brossa Gonzalo⁵³, D. Brundu^{25,45}, E. Buchanan⁵¹, A. Buonauro⁴⁷, C. Burr⁵⁹, A. Bursche²⁵, J.S. Butter³⁰, J. Buytaert⁴⁵, W. Byczynski⁴⁵, S. Cadeddu²⁵, H. Cai⁶⁹, R. Calabrese^{19,g}, S. Cali²¹, R. Calladine⁵⁰, M. Calvi^{23,i}, M. Calvo Gomez^{43,m}, A. Camboni^{43,m}, P. Campana²¹, D.H. Campora Perez⁴⁵, L. Capriotti^{18,e}, A. Carbone^{18,e}, G. Carboni²⁸, R. Cardinale^{22,h}, A. Cardini²⁵, P. Carniti^{23,i}, K. Carvalho Akiba³⁰, A. Casais Vidal⁴⁴, G. Casse⁵⁷, M. Cattaneo⁴⁵, G. Cavallero²², R. Cenci^{27,p}, M.G. Chapman⁵¹, M. Charles^{11,45}, Ph. Charpentier⁴⁵, G. Chatzikonstantinidis⁵⁰, M. Chefdeville⁷, V. Chekalina⁴⁰, C. Chen³, S. Chen²⁵, S.-G. Chitic⁴⁵, V. Chobanova⁴⁴, M. Chrzaszcz⁴⁵, A. Chubykin³⁶, P. Ciambone²¹, X. Cid Vidal⁴⁴, G. Ciezarek⁴⁵, F. Cindolo¹⁸, P.E.L. Clarke⁵⁵, M. Clemencic⁴⁵, H.V. Cliff⁵², J. Closier⁴⁵, J.L. Cobbedick⁵⁹, V. Coco⁴⁵, J.A.B. Coelho¹⁰, J. Cogan⁹, E. Cogneras⁸, L. Cojocariu³⁵, P. Collins⁴⁵, T. Colombo⁴⁵, A. Comerma-Montells¹⁵, A. Contu²⁵, G. Coombs⁴⁵, S. Coquereau⁴³, G. Corti⁴⁵, C.M. Costa Sobral⁵³, B. Couturier⁴⁵, G.A. Cowan⁵⁵, D.C. Craik⁶¹, A. Crocombe⁵³, M. Cruz Torres¹, R. Currie⁵⁵, C.L. Da Silva⁶⁴, E. Dall’Occo³⁰, J. Dalseno^{44,51}, C. D’Ambrosio⁴⁵, A. Danilina³⁷, P. d’Argent¹⁵, A. Davis⁵⁹, O. De Aguiar Francisco⁴⁵, K. De Bruyn⁴⁵, S. De Capua⁵⁹, M. De Cian⁴⁶, J.M. De Miranda¹, L. De Paula², M. De Serio^{17,d}, P. De Simone²¹, J.A. de Vries³⁰, C.T. Dean⁵⁶, W. Dean⁷⁸, D. Decamp⁷, L. Del Buono¹¹, B. Delaney⁵², H.-P. Dembinski¹⁴, M. Demmer¹³, A. Dendek³³, D. Derkach⁷⁵, O. Deschamps⁸, F. Desse¹⁰, F. Dettori²⁵, B. Dey⁶, A. Di Canto⁴⁵, P. Di Nezza²¹, S. Didenko⁷⁴, H. Dijkstra⁴⁵, F. Dordei²⁵, M. Dorigo^{27,x}, A.C. dos Reis¹, A. Dosil Suárez⁴⁴, L. Douglas⁵⁶, A. Dovbnya⁴⁸, K. Dreimanis⁵⁷, L. Dufour⁴⁵, G. Dujany¹¹, P. Durante⁴⁵, J.M. Durham⁶⁴, D. Dutta⁵⁹, R. Dzhelyadin^{42,†}, M. Dziewiecki¹⁵, A. Dziurda³², A. Dzyuba³⁶, S. Easo⁵⁴, U. Egede⁵⁸, V. Egorychev³⁷, S. Eidelman^{41,w}, S. Eisenhardt⁵⁵, U. Eitschberger¹³, R. Ekelhof¹³, S. Ek-In⁴⁶, L. Eklund⁵⁶, S. Ely⁶⁵, A. Ene³⁵, S. Escher¹², S. Esen³⁰, T. Evans⁶², A. Falabella¹⁸, C. Färber⁴⁵, N. Farley⁵⁰, S. Farry⁵⁷, D. Fazzini¹⁰, M. Féo⁴⁵, P. Fernandez Declara⁴⁵, A. Fernandez Prieto⁴⁴, F. Ferrari^{18,e}, L. Ferreira Lopes⁴⁶, F. Ferreira Rodrigues², S. Ferreres Sole³⁰, M. Ferro-Luzzi⁴⁵, S. Filippov³⁹, R.A. Fini¹⁷, M. Fiorini^{19,g}, M. Firlej³³, C. Fitzpatrick⁴⁵, T. Fiutowski³³, F. Fleuret^{10,b}, M. Fontana⁴⁵, F. Fontanelli^{22,h}, R. Forty⁴⁵, V. Franco Lima⁵⁷, M. Franco Sevilla⁶³, M. Frank⁴⁵, C. Frei⁴⁵, J. Fu^{24,q}, W. Funk⁴⁵, E. Gabriel⁵⁵, A. Gallas Torreira⁴⁴, D. Galli^{18,e}, S. Gallorini²⁶, S. Gambetta⁵⁵, Y. Gan³, M. Gandelman², P. Gandini²⁴, Y. Gao³, L.M. Garcia Martin⁷⁷, J. García Pardiñas⁴⁷, B. Garcia Plana⁴⁴, J. Garra Tico⁵², L. Garrido⁴³, D. Gascon⁴³, C. Gaspar⁴⁵, G. Gazzoni⁸, D. Gerick¹⁵, E. Gersabeck⁵⁹, M. Gersabeck⁵⁹, T. Gershon⁵³, D. Gerstel⁹, Ph. Ghez⁷, V. Gibson⁵², O.G. Girard⁴⁶, P. Gironella Gironell⁴³, L. Giubega³⁵,

K. Gizdov⁵⁵, V.V. Gligorov¹¹, C. Göbel⁶⁷, D. Golubkov³⁷, A. Golutvin^{58,74}, A. Gomes^{1,a},
 I.V. Gorelov³⁸, C. Gotti^{23,i}, E. Govorkova³⁰, J.P. Grabowski¹⁵, R. Graciani Diaz⁴³,
 L.A. Granado Cardoso⁴⁵, E. Graugés⁴³, E. Graverini⁴⁶, G. Graziani²⁰, A. Grecu³⁵, R. Greim³⁰,
 P. Griffith²⁵, L. Grillo⁵⁹, L. Gruber⁴⁵, B.R. Gruberg Cazon⁶⁰, C. Gu³, E. Gushchin³⁹,
 A. Guth¹², Yu. Guz^{42,45}, T. Gys⁴⁵, T. Hadavizadeh⁶⁰, C. Hadjivasiliou⁸, G. Haefeli⁴⁶,
 C. Haen⁴⁵, S.C. Haines⁵², P.M. Hamilton⁶³, Q. Han⁶, X. Han¹⁵, T.H. Hancock⁶⁰,
 S. Hansmann-Menzemer¹⁵, N. Harnew⁶⁰, T. Harrison⁵⁷, C. Hasse⁴⁵, M. Hatch⁴⁵, J. He⁴,
 M. Hecker⁵⁸, K. Heijhoff³⁰, K. Heinicke¹³, A. Heister¹³, K. Hennessy⁵⁷, L. Henry⁷⁷, M. Heß⁷¹,
 J. Heuel¹², A. Hicheur⁶⁶, R. Hidalgo Charman⁵⁹, D. Hill⁶⁰, M. Hilton⁵⁹, P.H. Hopchev⁴⁶,
 J. Hu¹⁵, W. Hu⁶, W. Huang⁴, Z.C. Huard⁶², W. Hulsbergen³⁰, T. Humair⁵⁸, M. Hushchyn⁷⁵,
 D. Hutchcroft⁵⁷, D. Hynds³⁰, P. Ibis¹³, M. Idzik³³, P. Ilten⁵⁰, A. Inglessi³⁶, A. Inyakin⁴²,
 K. Ivshin³⁶, R. Jacobsson⁴⁵, S. Jakobsen⁴⁵, J. Jalocha⁶⁰, E. Jans³⁰, B.K. Jashal⁷⁷,
 A. Jawahery⁶³, F. Jiang³, M. John⁶⁰, D. Johnson⁴⁵, C.R. Jones⁵², C. Joram⁴⁵, B. Jost⁴⁵,
 N. Jurik⁶⁰, S. Kandybei⁴⁸, M. Karacson⁴⁵, J.M. Kariuki⁵¹, S. Karodia⁵⁶, N. Kazeev⁷⁵,
 M. Kecke¹⁵, F. Keizer⁵², M. Kelsey⁶⁵, M. Kenzie⁵², T. Ketel³¹, B. Khanji⁴⁵, A. Kharisova⁷⁶,
 C. Khurewathanakul⁴⁶, K.E. Kim⁶⁵, T. Kirn¹², V.S. Kirsebom⁴⁶, S. Klaver²¹,
 K. Klimaszewski³⁴, S. Koliiev⁴⁹, M. Kolpin¹⁵, A. Kondybayeva⁷⁴, A. Konoplyannikov³⁷,
 P. Kopciwicz³³, R. Kopecna¹⁵, P. Koppenburg³⁰, I. Kostiuk^{30,49}, O. Kot⁴⁹, S. Kotriakhova³⁶,
 M. Kozeiha⁸, L. Kravchuk³⁹, M. Kreps⁵³, F. Kress⁵⁸, S. Kretzschmar¹², P. Krokovny^{41,w},
 W. Krupa³³, W. Krzemien³⁴, W. Kucewicz^{32,l}, M. Kucharczyk³², V. Kudryavtsev^{41,w},
 G.J. Kunde⁶⁴, A.K. Kuonen⁴⁶, T. Kvaratskheliya³⁷, D. Lacarrere⁴⁵, G. Lafferty⁵⁹, A. Lai²⁵,
 D. Lancierini⁴⁷, G. Lanfranchi²¹, C. Langenbruch¹², T. Latham⁵³, C. Lazzeroni⁵⁰, R. Le Gac⁹,
 R. Lefèvre⁸, A. Leflat³⁸, F. Lemaitre⁴⁵, O. Leroy⁹, T. Lesiak³², B. Leverington¹⁵, H. Li⁶⁸,
 P.-R. Li^{4,aa}, X. Li⁶⁴, Y. Li⁵, Z. Li⁶⁵, X. Liang⁶⁵, T. Likhomanenko⁷³, R. Lindner⁴⁵,
 F. Lionetto⁴⁷, V. Lisovskyi¹⁰, G. Liu⁶⁸, X. Liu³, D. Loh⁵³, A. Loi²⁵, J. Lomba Castro⁴⁴,
 I. Longstaff⁵⁶, J.H. Lopes², G. Loustau⁴⁷, G.H. Lovell⁵², D. Lucchesi^{26,o}, M. Lucio Martinez⁴⁴,
 Y. Luo³, A. Lupato²⁶, E. Luppi^{19,g}, O. Lupton⁵³, A. Lusiani^{27,t}, X. Lyu⁴, F. Machefert¹⁰,
 F. Maciuc³⁵, V. Macko⁴⁶, P. Mackowiak¹³, S. Maddrell-Mander⁵¹, O. Maev^{36,45}, K. Maguire⁵⁹,
 D. Maisuzenko³⁶, M.W. Majewski³³, S. Malde⁶⁰, B. Malecki⁴⁵, A. Malinin⁷³, T. Maltsev^{41,w},
 H. Malygina¹⁵, G. Manca^{25,f}, G. Mancinelli⁹, D. Marangotto^{24,q}, J. Maratas^{8,v}, J.F. Marchand⁷,
 U. Marconi¹⁸, C. Marin Benito¹⁰, M. Marinangeli⁴⁶, P. Marino⁴⁶, J. Marks¹⁵, P.J. Marshall⁵⁷,
 G. Martellotti²⁹, L. Martinazzoli⁴⁵, M. Martinelli^{45,23,i}, D. Martinez Santos⁴⁴,
 F. Martinez Vidal⁷⁷, A. Massafferri¹, M. Materok¹², R. Matev⁴⁵, A. Mathad⁴⁷, Z. Mathe⁴⁵,
 V. Matiunin³⁷, C. Matteuzzi²³, K.R. Mattioli⁷⁸, A. Mauri⁴⁷, E. Maurice^{10,b}, B. Maurin⁴⁶,
 M. McCann^{58,45}, A. McNab⁵⁹, R. McNulty¹⁶, J.V. Mead⁵⁷, B. Meadows⁶², C. Meaux⁹,
 N. Meinert⁷¹, D. Melnychuk³⁴, M. Merk³⁰, A. Merli^{24,q}, E. Michielin²⁶, D.A. Milanes⁷⁰,
 E. Millard⁵³, M.-N. Minard⁷, O. Mineev³⁷, L. Minzoni^{19,g}, D.S. Mitzel¹⁵, A. Mödden¹³,
 A. Mogini¹¹, R.D. Moise⁵⁸, T. Mombächer¹³, I.A. Monroy⁷⁰, S. Monteil⁸, M. Morandin²⁶,
 G. Morello²¹, M.J. Morello^{27,t}, J. Moron³³, A.B. Morris⁹, R. Mountain⁶⁵, H. Mu³, F. Muheim⁵⁵,
 M. Mukherjee⁶, M. Mulder³⁰, D. Müller⁴⁵, J. Müller¹³, K. Müller⁴⁷, V. Müller¹³,
 C.H. Murphy⁶⁰, D. Murray⁵⁹, P. Naik⁵¹, T. Nakada⁴⁶, R. Nandakumar⁵⁴, A. Nandi⁶⁰,
 T. Nanut⁴⁶, I. Nasteva², M. Needham⁵⁵, N. Neri^{24,q}, S. Neubert¹⁵, N. Neufeld⁴⁵,
 R. Newcombe⁵⁸, T.D. Nguyen⁴⁶, C. Nguyen-Mau^{46,n}, S. Nieswand¹², R. Niet¹³, N. Nikitin³⁸,
 N.S. Nolte⁴⁵, A. Oblakowska-Mucha³³, V. Obraztsov⁴², S. Ogilvy⁵⁶, D.P. O'Hanlon¹⁸,
 R. Oldeman^{25,f}, C.J.G. Onderwater⁷², J. D. Osborn⁷⁸, A. Ossowska³², J.M. Otalora Goicochea²,
 T. Ovsiannikova³⁷, P. Owen⁴⁷, A. Oyanguren⁷⁷, P.R. Pais⁴⁶, T. Pajero^{27,t}, A. Palano¹⁷,
 M. Palutan²¹, G. Panshin⁷⁶, A. Papanestis⁵⁴, M. Pappagallo⁵⁵, L.L. Pappalardo^{19,g},
 W. Parker⁶³, C. Parkes^{59,45}, G. Passaleva^{20,45}, A. Pastore¹⁷, M. Patel⁵⁸, C. Patrignani^{18,e},
 A. Pearce⁴⁵, A. Pellegrino³⁰, G. Penso²⁹, M. Pepe Altarelli⁴⁵, S. Perazzini¹⁸, D. Pereima³⁷,
 P. Perret⁸, L. Pescatore⁴⁶, K. Petridis⁵¹, A. Petrolini^{22,h}, A. Petrov⁷³, S. Petrucci⁵⁵,

M. Petruzzo^{24,q}, B. Pietrzyk⁷, G. Pietrzyk⁴⁶, M. Pikies³², M. Pili⁶⁰, D. Pinci²⁹, J. Pinzino⁴⁵,
F. Pisani⁴⁵, A. Piucci¹⁵, V. Placinta³⁵, S. Playfer⁵⁵, J. Plews⁵⁰, M. Plo Casasus⁴⁴, F. Polci¹¹,
M. Poli Lener²¹, M. Poliakova⁶⁵, A. Poluektov⁹, N. Polukhina^{74,c}, I. Polyakov⁶⁵, E. Polcarpo²,
G.J. Pomery⁵¹, S. Ponce⁴⁵, A. Popov⁴², D. Popov⁵⁰, S. Poslavskii⁴², E. Price⁵¹, C. Prouve⁴⁴,
V. Pugatch⁴⁹, A. Puig Navarro⁴⁷, H. Pullen⁶⁰, G. Punzi^{27,p}, W. Qian⁴, J. Qin⁴, R. Quagliani¹¹,
B. Quintana⁸, N.V. Raab¹⁶, B. Rachwal³³, J.H. Rademacker⁵¹, M. Rama²⁷, M. Ramos Pernas⁴⁴,
M.S. Rangel², F. Ratnikov^{40,75}, G. Raven³¹, M. Ravonel Salzgeber⁴⁵, M. Reboud⁷, F. Redi⁴⁶,
S. Reichert¹³, F. Reiss¹¹, C. Remon Alepuz⁷⁷, Z. Ren³, V. Renaudin⁶⁰, S. Ricciardi⁵⁴,
S. Richards⁵¹, K. Rinnert⁵⁷, P. Robbe¹⁰, A. Robert¹¹, A.B. Rodrigues⁴⁶, E. Rodrigues⁶²,
J.A. Rodriguez Lopez⁷⁰, M. Roehrken⁴⁵, S. Roiser⁴⁵, A. Rollings⁶⁰, V. Romanovskiy⁴²,
A. Romero Vidal⁴⁴, J.D. Roth⁷⁸, M. Rotondo²¹, M.S. Rudolph⁶⁵, T. Ruf⁴⁵, J. Ruiz Vidal⁷⁷,
J.J. Saborido Silva⁴⁴, N. Sagidova³⁶, B. Saitta^{25,f}, V. Salustino Guimaraes⁶⁷, C. Sanchez Gras³⁰,
C. Sanchez Mayordomo⁷⁷, B. Sanmartin Sedes⁴⁴, R. Santacesaria²⁹, C. Santamarina Rios⁴⁴,
M. Santimaria^{21,45}, E. Santovetti^{28,j}, G. Sarpis⁵⁹, A. Sarti^{21,k}, C. Satriano^{29,s}, A. Satta²⁸,
M. Saur⁴, D. Savrina^{37,38}, S. Schael¹², M. Schellenberg¹³, M. Schiller⁵⁶, H. Schindler⁴⁵,
M. Schmelling¹⁴, T. Schmelzer¹³, B. Schmidt⁴⁵, O. Schneider⁴⁶, A. Schopper⁴⁵, H.F. Schreiner⁶²,
M. Schubiger³⁰, S. Schulte⁴⁶, M.H. Schune¹⁰, R. Schwemmer⁴⁵, B. Sciascia²¹, A. Sciubba^{29,k},
A. Semennikov³⁷, E.S. Sepulveda¹¹, A. Sergi^{50,45}, N. Serra⁴⁷, J. Serrano⁹, L. Sestini²⁶,
A. Seuthe¹³, P. Seyfert⁴⁵, M. Shapkin⁴², T. Shears⁵⁷, L. Shekhtman^{41,w}, V. Shevchenko⁷³,
E. Shmanin⁷⁴, B.G. Siddi¹⁹, R. Silva Coutinho⁴⁷, L. Silva de Oliveira², G. Simi^{26,o},
S. Simone^{17,d}, I. Skiba¹⁹, N. Skidmore¹⁵, T. Skwarnicki⁶⁵, M.W. Slater⁵⁰, J.G. Smeaton⁵²,
E. Smith¹², I.T. Smith⁵⁵, M. Smith⁵⁸, M. Soares¹⁸, L. Soares Lavra¹, M.D. Sokoloff⁶²,
F.J.P. Soler⁵⁶, B. Souza De Paula², B. Spaan¹³, E. Spadaro Norella^{24,q}, P. Spradlin⁵⁶,
F. Stagni⁴⁵, M. Stahl¹⁵, S. Stahl⁴⁵, P. Stefko⁴⁶, S. Stefkova⁵⁸, O. Steinkamp⁴⁷, S. Stemmle¹⁵,
O. Stenyakin⁴², M. Stepanova³⁶, H. Stevens¹³, S. Stone⁶⁵, S. Stracka²⁷, M.E. Stramaglia⁴⁶,
M. Straticiu³⁵, U. Straumann⁴⁷, S. Strovkov⁷⁶, J. Sun³, L. Sun⁶⁹, Y. Sun⁶³, K. Swientek³³,
A. Szabelski³⁴, T. Szumlak³³, M. Szymanski⁴, Z. Tang³, T. Tekampe¹³, G. Tellarini¹⁹,
F. Teubert⁴⁵, E. Thomas⁴⁵, M.J. Tilley⁵⁸, V. Tisserand⁸, S. T'Jampens⁷, M. Tobin⁵, S. Tolk⁴⁵,
L. Tomassetti^{19,g}, D. Tonelli²⁷, D.Y. Tou¹¹, E. Tournefier⁷, M. Traill⁵⁶, M.T. Tran⁴⁶,
A. Trisovic⁵², A. Tsaregorodtsev⁹, G. Tuci^{27,45,p}, A. Tully⁵², N. Tuning³⁰, A. Ukleja³⁴,
A. Usachov¹⁰, A. Ustyuzhanin^{40,75}, U. Uwer¹⁵, A. Vagner⁷⁶, V. Vagnoni¹⁸, A. Valassi⁴⁵,
S. Valat⁴⁵, G. Valenti¹⁸, M. van Beuzekom³⁰, H. Van Hecke⁶⁴, E. van Herwijnen⁴⁵,
C.B. Van Hulse¹⁶, J. van Tilburg³⁰, M. van Veghel³⁰, R. Vazquez Gomez⁴⁵,
P. Vazquez Regueiro⁴⁴, C. Vázquez Sierra³⁰, S. Vecchi¹⁹, J.J. Velthuis⁵¹, M. Veltri^{20,r},
A. Venkateswaran⁶⁵, M. Vernet⁸, M. Veronesi³⁰, M. Vesterinen⁵³, J.V. Viana Barbosa⁴⁵,
D. Vieira⁴, M. Vieites Diaz⁴⁴, H. Viemann⁷¹, X. Vilasis-Cardona^{43,m}, A. Vitkovskiy³⁰,
M. Vitti⁵², V. Volkov³⁸, A. Vollhardt⁴⁷, D. Vom Bruch¹¹, B. Voneki⁴⁵, A. Vorobyev³⁶,
V. Vorobyev^{41,w}, N. Voropaev³⁶, R. Waldi⁷¹, J. Walsh²⁷, J. Wang³, J. Wang⁵, M. Wang³,
Y. Wang⁶, Z. Wang⁴⁷, D.R. Ward⁵², H.M. Wark⁵⁷, N.K. Watson⁵⁰, D. Websdale⁵⁸, A. Weiden⁴⁷,
C. Weisser⁶¹, M. Whitehead¹², G. Wilkinson⁶⁰, M. Wilkinson⁶⁵, I. Williams⁵², M. Williams⁶¹,
M.R.J. Williams⁵⁹, T. Williams⁵⁰, F.F. Wilson⁵⁴, M. Winn¹⁰, W. Wislicki³⁴, M. Witek³²,
G. Wormser¹⁰, S.A. Wotton⁵², K. Wyllie⁴⁵, Z. Xiang⁴, D. Xiao⁶, Y. Xie⁶, H. Xing⁶⁸, A. Xu³,
L. Xu³, M. Xu⁶, Q. Xu⁴, Z. Xu⁷, Z. Xu³, Z. Yang³, Z. Yang⁶³, Y. Yao⁶⁵, L.E. Yeomans⁵⁷,
H. Yin⁶, J. Yu^{6,z}, X. Yuan⁶⁵, O. Yushchenko⁴², K.A. Zarebski⁵⁰, M. Zavertyaev^{14,c}, M. Zeng³,
D. Zhang⁶, L. Zhang³, S. Zhang³, W.C. Zhang^{3,y}, Y. Zhang⁴⁵, A. Zhelezov¹⁵, Y. Zheng⁴,
Y. Zhou⁴, X. Zhu³, V. Zhukov^{12,38}, J.B. Zonneveld⁵⁵, S. Zucchelli^{18,e}.

¹Centro Brasileiro de Pesquisas Físicas (CBPF), Rio de Janeiro, Brazil

²Universidade Federal do Rio de Janeiro (UFRJ), Rio de Janeiro, Brazil

³Center for High Energy Physics, Tsinghua University, Beijing, China

⁴University of Chinese Academy of Sciences, Beijing, China

- ⁵*Institute Of High Energy Physics (IHEP), Beijing, China*
- ⁶*Institute of Particle Physics, Central China Normal University, Wuhan, Hubei, China*
- ⁷*Univ. Grenoble Alpes, Univ. Savoie Mont Blanc, CNRS, IN2P3-LAPP, Annecy, France*
- ⁸*Université Clermont Auvergne, CNRS/IN2P3, LPC, Clermont-Ferrand, France*
- ⁹*Aix Marseille Univ, CNRS/IN2P3, CPPM, Marseille, France*
- ¹⁰*LAL, Univ. Paris-Sud, CNRS/IN2P3, Université Paris-Saclay, Orsay, France*
- ¹¹*LPNHE, Sorbonne Université, Paris Diderot Sorbonne Paris Cité, CNRS/IN2P3, Paris, France*
- ¹²*I. Physikalisches Institut, RWTH Aachen University, Aachen, Germany*
- ¹³*Fakultät Physik, Technische Universität Dortmund, Dortmund, Germany*
- ¹⁴*Max-Planck-Institut für Kernphysik (MPIK), Heidelberg, Germany*
- ¹⁵*Physikalisches Institut, Ruprecht-Karls-Universität Heidelberg, Heidelberg, Germany*
- ¹⁶*School of Physics, University College Dublin, Dublin, Ireland*
- ¹⁷*INFN Sezione di Bari, Bari, Italy*
- ¹⁸*INFN Sezione di Bologna, Bologna, Italy*
- ¹⁹*INFN Sezione di Ferrara, Ferrara, Italy*
- ²⁰*INFN Sezione di Firenze, Firenze, Italy*
- ²¹*INFN Laboratori Nazionali di Frascati, Frascati, Italy*
- ²²*INFN Sezione di Genova, Genova, Italy*
- ²³*INFN Sezione di Milano-Bicocca, Milano, Italy*
- ²⁴*INFN Sezione di Milano, Milano, Italy*
- ²⁵*INFN Sezione di Cagliari, Monserrato, Italy*
- ²⁶*INFN Sezione di Padova, Padova, Italy*
- ²⁷*INFN Sezione di Pisa, Pisa, Italy*
- ²⁸*INFN Sezione di Roma Tor Vergata, Roma, Italy*
- ²⁹*INFN Sezione di Roma La Sapienza, Roma, Italy*
- ³⁰*Nikhef National Institute for Subatomic Physics, Amsterdam, Netherlands*
- ³¹*Nikhef National Institute for Subatomic Physics and VU University Amsterdam, Amsterdam, Netherlands*
- ³²*Henryk Niewodniczanski Institute of Nuclear Physics Polish Academy of Sciences, Kraków, Poland*
- ³³*AGH - University of Science and Technology, Faculty of Physics and Applied Computer Science, Kraków, Poland*
- ³⁴*National Center for Nuclear Research (NCBJ), Warsaw, Poland*
- ³⁵*Horia Hulubei National Institute of Physics and Nuclear Engineering, Bucharest-Magurele, Romania*
- ³⁶*Petersburg Nuclear Physics Institute NRC Kurchatov Institute (PNPI NRC KI), Gatchina, Russia*
- ³⁷*Institute of Theoretical and Experimental Physics NRC Kurchatov Institute (ITEP NRC KI), Moscow, Russia, Moscow, Russia*
- ³⁸*Institute of Nuclear Physics, Moscow State University (SINP MSU), Moscow, Russia*
- ³⁹*Institute for Nuclear Research of the Russian Academy of Sciences (INR RAS), Moscow, Russia*
- ⁴⁰*Yandex School of Data Analysis, Moscow, Russia*
- ⁴¹*Budker Institute of Nuclear Physics (SB RAS), Novosibirsk, Russia*
- ⁴²*Institute for High Energy Physics NRC Kurchatov Institute (IHEP NRC KI), Protvino, Russia, Protvino, Russia*
- ⁴³*ICCUB, Universitat de Barcelona, Barcelona, Spain*
- ⁴⁴*Instituto Galego de Física de Altas Enerxías (IGFAE), Universidade de Santiago de Compostela, Santiago de Compostela, Spain*
- ⁴⁵*European Organization for Nuclear Research (CERN), Geneva, Switzerland*
- ⁴⁶*Institute of Physics, Ecole Polytechnique Fédérale de Lausanne (EPFL), Lausanne, Switzerland*
- ⁴⁷*Physik-Institut, Universität Zürich, Zürich, Switzerland*
- ⁴⁸*NSC Kharkiv Institute of Physics and Technology (NSC KIPT), Kharkiv, Ukraine*
- ⁴⁹*Institute for Nuclear Research of the National Academy of Sciences (KINR), Kyiv, Ukraine*
- ⁵⁰*University of Birmingham, Birmingham, United Kingdom*
- ⁵¹*H.H. Wills Physics Laboratory, University of Bristol, Bristol, United Kingdom*
- ⁵²*Cavendish Laboratory, University of Cambridge, Cambridge, United Kingdom*
- ⁵³*Department of Physics, University of Warwick, Coventry, United Kingdom*
- ⁵⁴*STFC Rutherford Appleton Laboratory, Didcot, United Kingdom*
- ⁵⁵*School of Physics and Astronomy, University of Edinburgh, Edinburgh, United Kingdom*

- ⁵⁶ *School of Physics and Astronomy, University of Glasgow, Glasgow, United Kingdom*
- ⁵⁷ *Oliver Lodge Laboratory, University of Liverpool, Liverpool, United Kingdom*
- ⁵⁸ *Imperial College London, London, United Kingdom*
- ⁵⁹ *Department of Physics and Astronomy, University of Manchester, Manchester, United Kingdom*
- ⁶⁰ *Department of Physics, University of Oxford, Oxford, United Kingdom*
- ⁶¹ *Massachusetts Institute of Technology, Cambridge, MA, United States*
- ⁶² *University of Cincinnati, Cincinnati, OH, United States*
- ⁶³ *University of Maryland, College Park, MD, United States*
- ⁶⁴ *Los Alamos National Laboratory (LANL), Los Alamos, United States*
- ⁶⁵ *Syracuse University, Syracuse, NY, United States*
- ⁶⁶ *Laboratory of Mathematical and Subatomic Physics, Constantine, Algeria, associated to ²*
- ⁶⁷ *Pontifícia Universidade Católica do Rio de Janeiro (PUC-Rio), Rio de Janeiro, Brazil, associated to ²*
- ⁶⁸ *South China Normal University, Guangzhou, China, associated to ³*
- ⁶⁹ *School of Physics and Technology, Wuhan University, Wuhan, China, associated to ³*
- ⁷⁰ *Departamento de Física, Universidad Nacional de Colombia, Bogota, Colombia, associated to ¹¹*
- ⁷¹ *Institut für Physik, Universität Rostock, Rostock, Germany, associated to ¹⁵*
- ⁷² *Van Swinderen Institute, University of Groningen, Groningen, Netherlands, associated to ³⁰*
- ⁷³ *National Research Centre Kurchatov Institute, Moscow, Russia, associated to ³⁷*
- ⁷⁴ *National University of Science and Technology "MISIS", Moscow, Russia, associated to ³⁷*
- ⁷⁵ *National Research University Higher School of Economics, Moscow, Russia, associated to ⁴⁰*
- ⁷⁶ *National Research Tomsk Polytechnic University, Tomsk, Russia, associated to ³⁷*
- ⁷⁷ *Instituto de Física Corpuscular, Centro Mixto Universidad de Valencia - CSIC, Valencia, Spain, associated to ⁴³*
- ⁷⁸ *University of Michigan, Ann Arbor, United States, associated to ⁶⁵*

^a *Universidade Federal do Triângulo Mineiro (UFTM), Uberaba-MG, Brazil*

^b *Laboratoire Leprince-Ringuet, Palaiseau, France*

^c *P.N. Lebedev Physical Institute, Russian Academy of Science (LPI RAS), Moscow, Russia*

^d *Università di Bari, Bari, Italy*

^e *Università di Bologna, Bologna, Italy*

^f *Università di Cagliari, Cagliari, Italy*

^g *Università di Ferrara, Ferrara, Italy*

^h *Università di Genova, Genova, Italy*

ⁱ *Università di Milano Bicocca, Milano, Italy*

^j *Università di Roma Tor Vergata, Roma, Italy*

^k *Università di Roma La Sapienza, Roma, Italy*

^l *AGH - University of Science and Technology, Faculty of Computer Science, Electronics and Telecommunications, Kraków, Poland*

^m *LIFAEELS, La Salle, Universitat Ramon Llull, Barcelona, Spain*

ⁿ *Hanoi University of Science, Hanoi, Vietnam*

^o *Università di Padova, Padova, Italy*

^p *Università di Pisa, Pisa, Italy*

^q *Università degli Studi di Milano, Milano, Italy*

^r *Università di Urbino, Urbino, Italy*

^s *Università della Basilicata, Potenza, Italy*

^t *Scuola Normale Superiore, Pisa, Italy*

^u *Università di Modena e Reggio Emilia, Modena, Italy*

^v *MSU - Iligan Institute of Technology (MSU-IIT), Iligan, Philippines*

^w *Novosibirsk State University, Novosibirsk, Russia*

^x *INFN Sezione di Trieste, Trieste, Italy*

^y *School of Physics and Information Technology, Shaanxi Normal University (SNNU), Xi'an, China*

^z *Physics and Micro Electronic College, Hunan University, Changsha City, China*

^{aa} *Lanzhou University, Lanzhou, China*

† *Deceased*